



CHARACTERIZATION OF MULTILAYER SUPERHYDROPHOBIC SURFACE FOR ENHANCED HIGH VOLTAGE INSULATION

SARA ALOUACHE¹, ABDELLAH MEDJDOUB¹, MURAT TOMAKIN²

Keywords: Superhydrophobic surface; Multilayer coating; Contact angle; Optical properties; Hydrophobicity enhancement; High voltage insulation.

Superhydrophobic surfaces are widely used in electrical systems to repel moisture and enhance insulation performance. However, their exposure to environmental contaminants can degrade them over time. This study aims to characterize the properties of additional layers by analyzing their optical and structural characteristics. To evaluate the impact of multilayer deposition on their performance, several samples were prepared, then analyzed by FTIR, SEM, spectrometry, and contact angle measurement. The results indicate that increasing the number of layers enhances the structural uniformity, electrical stability, and optical transmission. These findings show the importance of multilayer structures in optimizing these surfaces, especially for electrical insulation.

1. INTRODUCTION

Superhydrophobicity, inspired by natural phenomena, refers to surfaces or materials that exhibit water-repellent properties [1,2], particularly in organisms such as lotus leaves [3], Gerris [4], fish scales [5], and butterfly wings [6]. Superhydrophobic surfaces have attracted considerable interest due to their non-wetting properties, characterized by a contact angle with the substrate greater than 150° , which complicates water adhesion [7]. Due to their self-cleaning, anti-icing, and anti-corrosion properties, these materials are utilized across diverse applications [8,9]. In electrical engineering, superhydrophobic surfaces are used in high-voltage electrical insulators to optimize the efficiency and durability of these components in electrical systems [10].

All electrical insulation materials, including superhydrophobic surfaces, can be adversely affected by environmental conditions over extended use. Héctor et al. [11] found that these coatings degrade and lose their hydrophobicity with prolonged exposure, thereby diminishing their effectiveness in electrical systems. Several studies in high-voltage engineering have demonstrated that insulating materials are significantly affected by aging, leakage currents, and surface discharges, which can undermine their long-term reliability [12,13].

To mitigate contamination risk in electrical insulators, numerous studies have investigated the application of superhydrophobic surfaces [14,15]. He et al. [16] utilized a spraying technique to create superhydrophobic surfaces after analyzing the distribution characteristics of water droplets on these surfaces through direct condensation tests and simulation studies. Their findings revealed that the distance between the droplets and the high contact angle increases the breakdown voltage of the surfaces under polluted conditions.

Arshad et al [17] have carried out a study on the properties and applications of superhydrophobic surfaces in high-voltage insulators, highlighting the degradation mechanism of these surfaces, which will enable researchers to optimize the performance and durability of superhydrophobic surfaces. Anahita et al [18] aim to develop a superhydrophobic coating to extend the service life of high-voltage insulators. A comparison of the electrical properties of this coating with those of bare porcelain under different environmental conditions showed an improvement in breakdown voltage and a reduction in leakage current measured during the condensation test on superhydrophobic surfaces. These observations align with

recent studies on insulation diagnostics and lifetime predictions in high-voltage equipment [19], highlighting the need to enhance insulating surfaces for outdoor applications.

Thus, studies on the evolution of superhydrophobic surfaces are still underway to improve their performance and durability, which remains a complex task that poses significant challenges.

Several methods have been used by many researchers to produce and improve superhydrophobic surfaces which are often limited to a surface to single-layer coatings [18,21], these different techniques can influence or modify the composition and state of the surface [20–22], to obtain a high state of hydrophobicity it is important to gain a deep understanding of the morphological, optical, chemical and also electrical characteristics of superhydrophobic surfaces. In particular, understand the impact of their property modifications on the evolution of the state and performance of superhydrophobic surfaces.

This study aims to characterize multilayer superhydrophobic coatings through various experimental techniques. Scanning electron microscopy (SEM), Fourier transform infrared spectroscopy (FTIR), photoluminescence, chemical composition, optical properties, and contact angle measurement to evaluate these results. This analysis will establish a direct correlation between the materials' microstructure and their functional properties, facilitating the development of strategies for adaptation to diverse industrial applications.

2. MATERIALS AND METHODS

2.1 FABRICATION OF SUPERHYDROPHOBIC SURFACES

The multilayer superhydrophobic surfaces were designed using a commercial silicone gel, Quilosa AkLISIL. The first layer was deposited by manually spreading a small amount of silicone gel, forming a thin and uniform layer on a glass plate with dimensions of $5 \times 5 \times 0.5$ cm. An uncontrolled quantity of the same silicone gel was burned, and the glass plate coated with fresh gel was then exposed to the flame in a uniform manner until the surface was completely blackened, thus forming a soot coating. The sample was cleaned with water to remove fragile soot residue. Subsequent layers were applied following the same procedure, with a 24-hour interval between each application. The obtained surface is about a few micrometers in thickness, as given by the MEB.

¹University A. Mira of Bejaia, Faculty of Technology, Laboratory of Electrical Engineering, 06000, Bejaia, Algeria.

²Department of Physics, Recep Tayyip Erdogan University, Rize, 53100, Turkey.

E-mails: sara.alouache@univ-bejaia, dzabdellah.medjdoub@univ-bejaia, dzmurat.tomakin@erdogan.edu.tr

2.2 SURFACE CHARACTERIZATION

2.2.1 CONTACT ANGLE MEASUREMENT

The contact angle measurement is regarded as the main indicator of the surface condition and the level of superhydrophobicity. Using a goniometer, the contact angle of multilayer superhydrophobic surfaces was measured to evaluate the variation of this property with the increase in the number of coating layers applied.

2.2.2 FTIR (FOURIER-TRANSFORM INFRARED SPECTROSCOPY)

The surface's chemical composition was analyzed using Fourier transform infrared spectrometry with a Perkin Elmer Spectrum100 spectrometer, operating in the range of 400-4000 cm^{-1} . Data were collected via the Spectrum software after a single scan sample.

2.2.3 SEM (SCANNING ELECTRON MICROSCOPY)

Scanning electron microscopy (SEM) (JEOL JSM-6610) was employed to analyze the morphological and topological characteristics of multilayer superhydrophobic surfaces, focusing on asperity morphology and roughness. An acceleration voltage of 15 kV was utilized across varying structural magnifications.

A cross-section was obtained by tilting the samples at 45° to assess the evolution of surface thickness with increasing number of superhydrophobic coatings.

2.2.4 PHOTOLUMINESCENCE

Optical characterization of superhydrophobic multilayer surfaces was carried out by room-temperature photoluminescence (RTPL) analysis using a Dong Woo Opton device fitted with an Xe lamp operating at 450 W in the 400- 900 nm wavelength range, with 350 nm excitation.

3. RESULTS AND DISCUSSION

3.1 SURFACE WETTABILITY

Numerous studies, including those by [23], have established that the contact angle is one of the most relevant indicators for characterizing the wettability and superhydrophobicity of a surface. In this study, a series of contact angle measurements was performed on superhydrophobic surfaces coated with a varying number of layers, to monitor the evolution of this parameter as a function of the number of successive deposits.

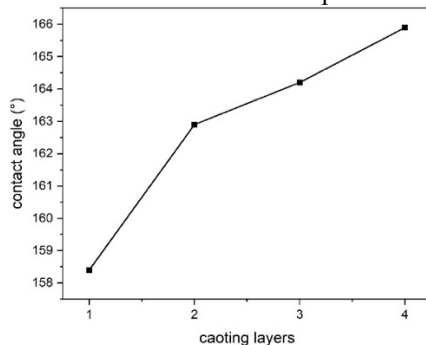


Fig. 1 – Vontact angle evolution for multilayer superhydrophobic surfaces ($V = 50 \mu\text{L}$).

As shown in Fig. 1, the contact angle notably increases with the addition of each further layer. This rises from 158.4° for a single-layer surface to 165.9° for a four-layer sample. This trend clearly demonstrates an enhancement in hydrophobic

behavior, confirming that adding more coating layers effectively improves the surface's superhydrophobicity.

3.2 CHEMICAL ANALYSIS

Figure 2 illustrates the FTIR spectra of superhydrophobic surfaces as a function of coating layer count, ranging from 1 to 4. The principal peaks across all spectra indicate stable chemical functional groups, with intensities varying based on the number of layers.

Absorption peaks between 2900 cm^{-1} and 3000 cm^{-1} correspond to the stretching vibrations of C-H bonds in the alkyl groups of hydrophobic compounds. Peaks between 1400 cm^{-1} and 1600 cm^{-1} , associated with C-H and C-C bond vibrations, further confirm the presence of alkyl groups. In the 1000 cm^{-1} to 1100 cm^{-1} range, typically linked to Si-O-Si bond stretching vibrations, the emergence of this band signifies the formation of a silica network, essential for the coating's mechanical stability. The band around 760 cm^{-1} is attributed to out-of-plane deformations of Si-O or C-H groups.

FTIR analysis indicates a slight increase in the intensity of the O-H and Si-O-Si bands with an increasing number of layers, suggesting enhanced superhydrophobicity and improved surface density and structure.

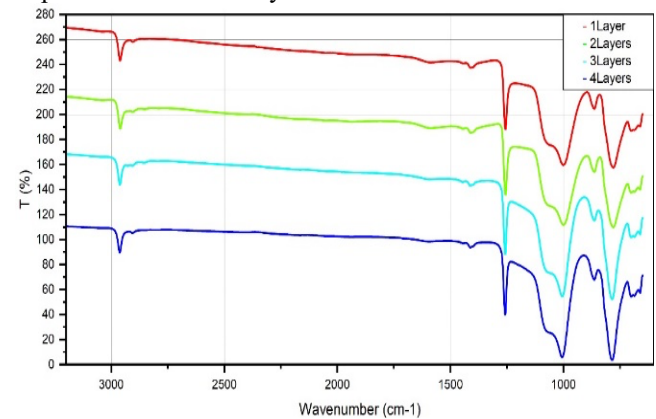


Fig. 2 – FTIR spectra of superhydrophobic surfaces.

3.3 MORPHOLOGICAL ANALYSIS

The surface condition and superhydrophobicity are determined by the roughness and morphology of the applied coatings. Figure 5 presents the macroscopic structures of superhydrophobic surfaces, with several layers ranging from 1 to 4 at different magnification scales to analyze various aspects of these surfaces.

At low magnification, the overall structure of asperities becomes visible, revealing a less dense distribution of particles on a single coating layer, resulting in low roughness. Adding a second coating layer significantly increases the density of asperities, thereby enhancing the surface hydrophobicity by creating additional sites capable of trapping air, which is an essential criterion for achieving superhydrophobicity. The third layer produces a more homogeneous and dense structure with a uniform distribution of particles (asperities), thus achieving an optimal roughness level to promote superhydrophobicity. In contrast, the addition of a fourth layer shows a structure like that observed with three layers.

At higher magnification levels, the morphology and finer details of individual asperities are more distinctly observed, allowing for precise and comprehensive surface characterization. This demonstrates that with an increasing

number of coating layers, surface roughness and asperity distribution achieve greater uniformity, reaching optimal conditions.

A direct correlation is evident between asperity density, distribution, and the superhydrophobic properties of the surface, depending on the number of applied coating layers.

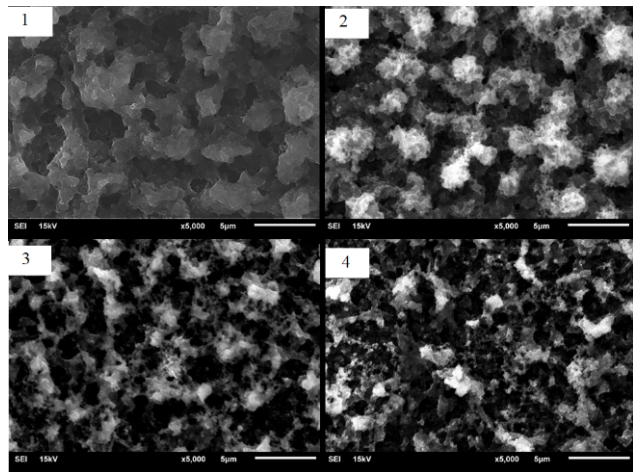
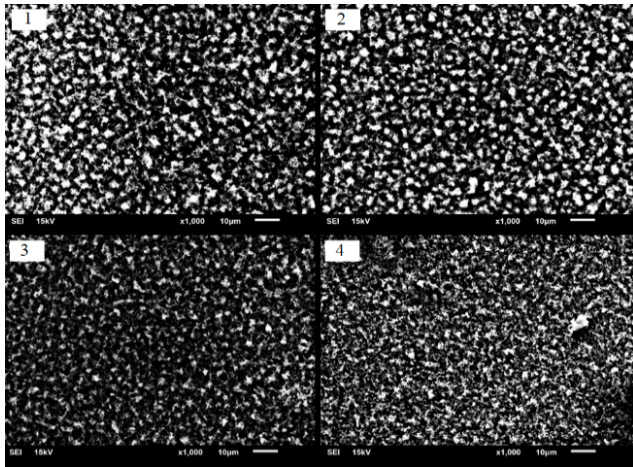


Fig. 3 – SEM observation of the morphology of multilayer superhydrophobic surfaces.

Cross-sectional SEM analysis of superhydrophobic coating layers allows us to follow the evolution of surface thickness, Tables 1 and 2.

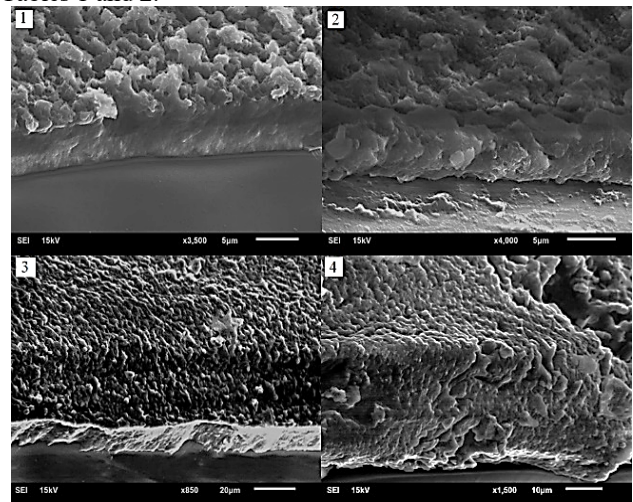


Fig. 4 – Thickness evolution of superhydrophobic multilayer coatings (1 to 4 layers).

Figure 4 shows a progressive increase in the thickness and particle density of superhydrophobic coatings with the addition of further layers. The first layer has a minimum thickness with irregular variations between 3.9 μm and 5.1 μm , and a low density of asperities. The successive addition of layers 2 and 3 leads to an increase in surface roughness with a notable rise in thickness. The fourth layer has a saturated structure with a less marked increase than the previous layers and a continuous increase in surface thickness in the range 23.7 μm to 25.7 μm .

Table 1

Thickness evolution of the multilayer superhydrophobic surface.

1 coating layer	2 coating layers	3 coating layers	4 coating layers
3.9 μm	4.3 μm	7.7 μm	23.7 μm
4.5 μm	4.6 μm	9.1 μm	24 μm
4.9 μm	5.04 μm	10.8 μm	24.6 μm
5.1 μm	5.5 μm	11.3 μm	25.7 μm

Table 2

Thickness of multilayers superhydrophobic surface (1 to 4 layers).

Number of Layers	Thickness
1 layer	4.6 μm
2 layers	4.9 μm
3 layers	9.7 μm
4 layers	24.5 μm

SEM analysis was employed to determine the chemical composition of superhydrophobic surfaces across varying layer counts.

Figure 5 presents the results of a three-point elemental analysis on a superhydrophobic surface. The EDS spectra for each point reveal the intensity of key elements detected: carbon (C), oxygen (O), and silicon (Si). Peak intensities for these elements are almost similar for all three points, suggesting the homogeneity and uniformity of the surface. Carbon composition appears to dominate in all spectra, while oxygen and silicon exhibit lower intensities.

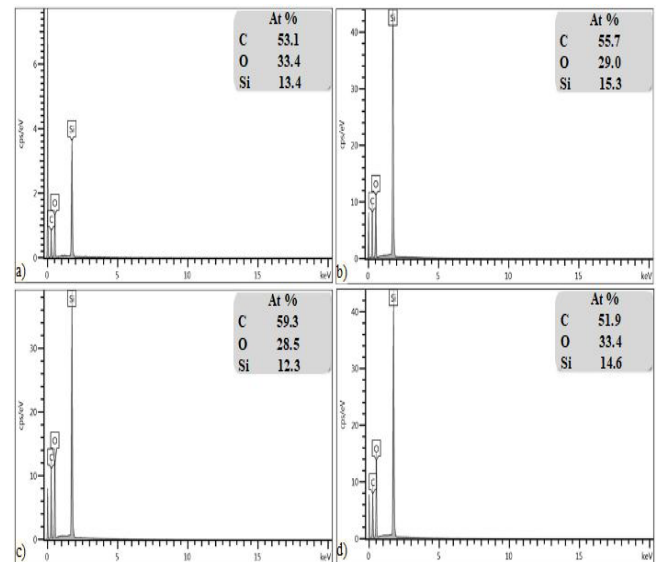


Fig. 5 – SEM analysis of chemical composition variations of multilayer superhydrophobic surfaces: a) 1 layer, b) 2 layers, c) 3 layers, d) 4 layers.

Table 3 shows the evolution of three chemical components: carbon (C), oxygen (O), and silicon (Si) in samples with varying numbers of coating layers.

Table 3

Atomic percentages obtained by EDS spectroscopy for multilayer superhydrophobic surfaces

Chemical element	Atomic percentages (AT%)			
	1 Layer	2 Layers	3 Layers	4 Layers
C	53.1	55.7	59.3	51.9
O	33.4	29.0	28.5	33.4
Si	13.4	15.3	12.3	14.6

The carbon content, associated with hydrophobic surface groups, increases from 53.1% to 59.3% across three coating layers, indicating enhanced superhydrophobicity. This trend is explained by the commonly observed correlation between higher carbon concentration and higher density of hydrophobic functional groups such as C-H and C-C bonds. However, a slight decrease in carbon content is observed in the fourth coating layer, attributed to surface saturation due to changes in the composition and distribution of carbon at the surface.

At the same time, the oxygen content decreases from 33.4% with one layer to 28.5% with three layers, suggesting a reduction in polar groups (O-H), which are generally responsible for hydrophilic behavior. It is noteworthy that the oxygen content increases again to 33.4% with the fourth layer, suggesting a partial reappearance of polar groups or a modification of the surface chemistry due to the overcoating.

The analysis of the silicon (Si) component shows a relatively stable variation over the four layers. This element plays a key role in the formation of hydrophobic Si-O-Si bonds, which contribute to the progressive transformation of the surface structure into a hydrophobic state as the coating layers accumulate.

Overall, the increase in carbon content combined with the decrease in oxygen up to three layers confirms an improvement in surface hydrophobicity and stability. However, the slight reversal observed with the fourth layer suggests that beyond a certain threshold, the addition of further layers may lead to a chemical imbalance.

SEM/EDS analysis established a direct correlation between the local chemical composition and the surface electrical properties [24].

3.4 OPTICAL PROPERTIES

Figure 6 presents the photoluminescence results for superhydrophobic surfaces with coating layers varying from 1 to 4. The profiles obtained exhibit distinct peak shapes and positions, which serve as significant indicators for identifying potential surface defects. This conclusion is drawn from an analysis of variations in the shape and position of peaks associated with surface functional groups. Notably, there is a pronounced variation in photoluminescence (PL) intensity in relation to the number of layers, while both peak position and shape remain consistent with the addition of further layers.

These findings suggest a stable homogeneity, a consistent density of electronic states, and optical stability in superhydrophobic surfaces with the incorporation of additional layers. This configuration also has the potential to enhance electrical properties, thereby improving insulation and durability [25,26].

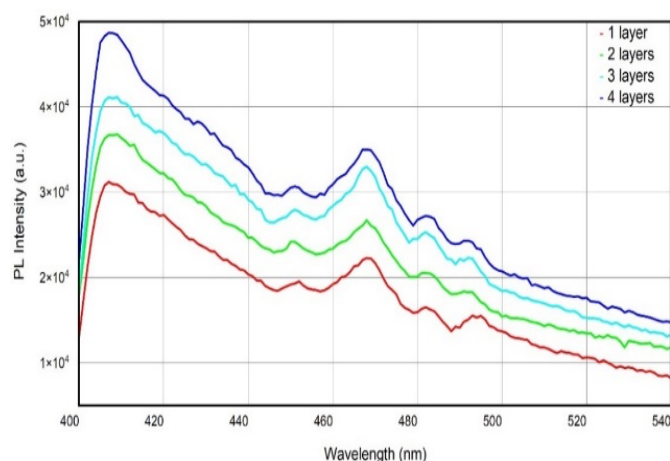


Fig. 6 – PL plots of multilayer superhydrophobic surface.

4. CONCLUSION

The overall results demonstrated a significant improvement in the wettability of superhydrophobic surfaces. Contact angle measurements showed a progressive increase with the growing number of coating layers, reaching values exceeding 150°. This enhancement is attributed to both the surface roughness and its chemical composition. FTIR analyses revealed a strong presence of Si-O-Si functional groups, with increasing intensity, indicating the chemical stability of the surfaces as the number of layers increases. Furthermore, SEM images highlighted an increase in roughness due to the superposition of layers, which promotes air entrapment at the interface in accordance with the Cassie-Baxter model. This structure was confirmed by EDS analyses, which showed a homogeneous distribution of oxygen and silicon across the surfaces. The consistent position and intensity of the PL peaks indicate a stable surface structure that contributes to superhydrophobic performance.

Therefore, the multilayer configuration emerges as a promising and effective strategy for enhancing the chemical, morphological, and optical properties of superhydrophobic surfaces.

CREDIT AUTHORSHIP CONTRIBUTION STATEMENT

SARA ALOUACHE: Investigation (experimental work, Validation, results treatment), methodology, writing – original draft, writing – review & editing.

ABDELLAH MEDJDOUB: Supervision, review & editing.

MURAT TOMAKIN: resources (laboratory and equipment), investigation (experimental tests), review & editing.

Received on August 27, 2025

REFERENCES

1. P. Roach, N.J. Shirtcliffe, M.I. Newton, *Progress in superhydrophobic surface development*, *Soft Matter*, **4**, 2, pp. 224–240 (2008).
2. G. Wang, A. Li, W. Zhao, Z. Xu, Y. Ma, F. Zhang, L. Qiao, C. Zhang, Q. He, *A review on fabrication methods and research progress of superhydrophobic silicone rubber materials*, *Advanced Materials Interfaces*, **8**, 1, pp. 1–15 (2021).
3. X. He, S. Ren, R. Tong, *The preparation of a superhydrophobic fluorine rubber surface*, *Coatings*, **12**, 12, pp. 1–10 (2022).
4. Z. Tang, B. Xu, X. Man, H. Liu, *Bioinspired superhydrophobic fibrous materials*, *Small Methods*, **8**, 4, pp. 1–15 (2024).
5. Y. Wang, Z. Zhang, J. Xu, H. Yu, *One-step method using laser for large-scale preparation of bionic superhydrophobic & drag-*

- reducing fish-scale surface*, Surface and Coatings Technology, **409**, pp. 1–8 (2021).
6. Z. Chen, Z. Zhang, Y. Wang, D. Xu, Y. Zhao, *Butterfly-inspired functional materials*, Mater. Sci. Eng. R Rep., **144**, pp. 1–15 (2021).
 7. A.R. Esmacili, N. Mir, R. Mohammadi, *A facile, fast, and low-cost method for fabrication of micro/nano-textured superhydrophobic surfaces*, J. Colloid Interface Sci., **573**, pp. 317–327 (2020).
 8. Z. Li, X. Wang, H. Bai, M. Cao, *Advances in bioinspired superhydrophobic surfaces made from silicones: Fabrication and application*, Polymers, **15**, 3, pp. 1–20 (2023).
 9. Z. Bai, J. Zhu, *A facile preparation method for corrosion-resistant copper superhydrophobic surfaces with ordered microstructures by etching*, Coatings, **13**, 7, pp. 1–12 (2023).
 10. R.A. Ghunem, E.A. Cherney, M. Farzaneh, G. Momen, H.A. Illias, G.A.M. Malagón, F. Yin, *Development and application of superhydrophobic outdoor insulation: A review*, IEEE Transactions on Dielectrics and Electrical Insulation, **29**, 4, pp. 1392–1399 (2022).
 11. H. de Santos, M.Á. Sanz-Bobi, *Research on the pollution performance and degradation of superhydrophobic nano-coatings for toughened glass insulators*, Electric Power Systems Research, **191**, pp. 1–9 (2021).
 12. O. Gubarevych, S. Goolak, S. Golubieva, *Systematization and selection of diagnosing methods for the stator windings insulation of induction motors*, Rev. Roum. Sci. Techn. – Électrotechn. et Énerg., **67**, 4, pp. 445–450 (2022).
 13. S.Y. Cherif, D. Benoudjit, M.S. Nait-Said, N. Nait-Said, *Incipient short-circuit fault impact on service continuity of an electric vehicle propelled by dual induction motors structure*, Rev. Roum. Sci. Techn. – Électrotechn. et Énerg., **67**, 3, pp. 265–270 (2022).
 14. W. Peng, X. Gou, H. Qin, M. Zhao, X. Zhao, Z. Guo, *Robust Mg(OH)₂/epoxy resin superhydrophobic coating applied to composite insulators*, Applied Surface Science, **466**, pp. 126–132 (2019).
 15. S. Alouache, F. Bouchelga, K. Hamour, *Simulation of electrical field and potential on multilayer superhydrophobic insulation with water drops under DC voltage*, 2nd International Conference on Advanced Electrical Engineering (ICAEE), Constantine, Algeria, pp. 1–6 (2022).
 16. Y. He, Y. Yang, X. Guo, H. Xia, *Condensation test and simulation of superhydrophobic coatings*, Coatings, **9**, 11, pp. 1–10 (2019).
 17. G. Arshad, M. Momen, S. Farzaneh, A. Nekahi, *Properties and applications of superhydrophobic coatings in high voltage outdoor insulation: A review*, IEEE Trans. Dielectr. Electr. Insul., **24**, 1, pp. 519–528 (2017).
 18. A. Allahdini, G. Momen, F. Munger, S. Brettschneider, I. Fofana, R. Jafari, *Performance of a nanotextured superhydrophobic coating developed for high-voltage outdoor porcelain insulators*, Colloids and Surfaces A: Physicochemical and Engineering Aspects, **649**, pp. 1–10 (2022).
 19. K. Guerraiche, A.B. Abbou, L. Dekhici, *Intelligent fault detection and location in electrical high-voltage transmission lines*, Rev. Roum. Sci. Techn. – Électrotechn. et Énerg., **69**, 3, pp. 269–276 (2024).
 20. S.A. Seyedmehdi, H. Zhang, J. Zhu, *Influence of production method, silicone type and thickness on silicon rubber superhydrophobic coatings*, Prog. Org. Coat., **90**, pp. 291–295 (2016).
 21. A.C. Ribeiro, B.G. Soares, J.G.M. Furtado, A.A. Silva, N.S.S.E. Couto, *Superhydrophobic nanocomposite coatings based on different polysiloxane matrices designed for electrical insulators*, Prog. Org. Coat., **168**, pp. 1–10 (2022).
 22. S. Alouache, A. Medjdoub, *Improving electrical performance of multilayer superhydrophobic coating for high voltage application*, J. Electr. Syst., **21**, 1, pp. 1–8 (2025).
 23. C. Mortier, *Conception de surfaces bio-inspirées à mouillabilité contrôlée à partir de polymères conducteurs*, Doctoral dissertation, COMUE Université Côte d’Azur, France, pp. 1–200 (2017).
 24. M.V. Lungu, A. Caramitu, M. Marin, D. Pătroi, V. Marinescu, C. Manea, A. Barbu, *Performance of zinc oxide-vanadium pentoxide varistors in medium voltage surge arresters*, Rev. Roum. Sci. Techn. – Électrotechn. et Énerg., **69**, 2, pp. 183–188 (2024).
 25. M.U.M. Junaidi, S.H. Azaman, N.N.R. Ahmad, C.P. Leo, G.W. Lim, D.J.C. Chan, H.M. Yee, *Superhydrophobic coating of silica with photoluminescence properties synthesized from rice husk ash*, Prog. Org. Coat., **111**, pp. 29–37 (2017).
 26. G.O. Piret, *Nanofils de silicium pour analyse sensible de biomolécules par spectrométrie de masse et pour l’adressage fluide de cellules en vue des applications de laboratoire sur puce et biopuces*, Doctoral dissertation, Université des Sciences et Technologies de Lille, Lille I, France, pp. 1–250 (2010).